

High Yield Recombinant Expression, Characterization and Homology Modeling of Two Types of *Cis*-epoxysuccinic Acid Hydrolases

Gu-Zhen Cui · Shan Wang · Yifei Li ·
Yi-Jun Tian · Yingang Feng · Qiu Cui

Published online: 17 May 2012
© Springer Science+Business Media, LLC 2012

Abstract The *cis*-epoxysuccinate hydrolases (CESHs), members of epoxide hydrolase, catalyze *cis*-epoxysuccinic acid hydrolysis to form D(–)-tartaric acid or L(+)-tartaric acid which are important chemicals with broad scientific and industrial applications. Two types of CESHs (CESH[D] and CESH[L], producing D(–)- and L(+)-tartaric acids, respectively) have been reported with low yield and complicated purification procedure in previous studies. In this paper, the two CESHs were overexpressed in *Escherichia coli* using codon-optimized genes. High protein yields by one-step purifications were obtained for both recombinant enzymes. The optimal pH and temperature were measured for both recombinant CESHs, and the properties of recombinant enzymes were similar to native enzymes. Kinetics parameters measured by Lineweaver–Burk plot indicates both enzymes exhibited similar affinity to *cis*-epoxysuccinic acid, but CESH[L] showed much higher catalytic efficiency than CESH[D], suggesting that the two CESHs have different catalytic mechanisms. The structures of both CESHs constructed by homology modeling indicated that CESH[L] and CESH[D] have different structural folds and potential active site residues.

CESH[L] adopted a typical α/β -hydrolase fold with a cap domain and a core domain, whereas CESH[D] possessed a unique TIM barrel fold composed of 8 α -helices and 8 β -strands, and 2 extra short α -helices exist on the top and bottom of the barrel, respectively. A divalent metal ion, preferred to be zinc, was found in CESH[D], and the ion was proved to be crucial to the enzymatic activity. These results provide structural insight into the different catalytic mechanisms of the two CESHs.

Keywords *Cis*-epoxysuccinic acid hydrolase · Epoxide hydrolase · Enzyme kinetics · Protein characterization · Recombinant expression · Homology modeling

Abbreviations

CESH	<i>cis</i> -epoxysuccinate hydrolases
CESH[D]	The CESH producing D(–)-tartaric acid
CESH[L]	The CESH producing L(+)-tartaric acid
PDB	Protein Data Bank

Electronic supplementary material The online version of this article (doi:10.1007/s10930-012-9418-5) contains supplementary material, which is available to authorized users.

G.-Z. Cui · S. Wang · Y. Li · Y.-J. Tian · Y. Feng · Q. Cui (✉)
Shandong Provincial Key Laboratory of Energy Genetics,
Key Laboratory of Biofuels, Qingdao Institute of Bioenergy
and Bioprocess Technology, Chinese Academy of Sciences,
No. 189 Songling Road, Qingdao 266101, China
e-mail: cuiqiu@qibebt.ac.cn

G.-Z. Cui · S. Wang
Graduate School of the Chinese Academy of Sciences,
Beijing 100049, China

1 Introduction

Chiral epoxides and diols, which can be used to produce optically active chiral compounds, are important synthons in modern organic chemistry and pharmaceuticals [4, 13]. A major challenge to generate optically active chiral compounds is to find suitable catalysts which catalyze reactions with both high yields and high stereo- and regio-selectivities [13]. Recently, microbial epoxide hydrolases have received much attention as a biocatalyst for producing enantiopure epoxides from racemic epoxides with high yields and

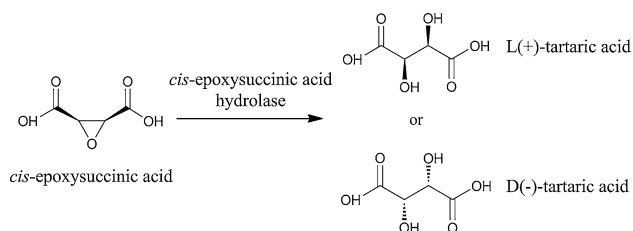


Fig. 1 Hydrolysis of *cis*-epoxysuccinic acid by *cis*-epoxysuccinic acid hydrolase to form D(–)- or L(+)-tartaric acid

selectivities [1, 2]. Epoxide hydrolase is a cofactor-independent, relatively stable and easy-to-use enzyme, which exists widely from bacteria to mammals [1, 9, 15, 27]. Preliminary data indicate that these enzymes belong structurally to the α/β -hydrolase fold family [26], but the structures of these enzymes are largely unknown.

The *cis*-epoxysuccinate hydrolases (CESHs) are epoxide hydrolase members which catalyze the hydrolysis of *cis*-epoxysuccinic acid to form D(–)-tartaric acid or L(+)-tartaric acid (Fig. 1) [16, 19, 21]. The enantiomeric tartaric acids, L(+)- and D(–)-tartaric acids, are well-known chiral chemicals with broad scientific and industrial applications [7, 11, 28]. The gene of several CESHs, for both CESH[D] and CESH[L], have been sequenced and cloned, and the enzymes were purified from the original species [16, 19, 21]. Both CESH[D] and CESH[L] had been cloned into *Escherichia coli* [19, 21], but no purification from *Escherichia coli* was reported in literature, and the yields of the purification from the original species were quite low. The low yield and complicated purification procedure may limit the structural/biochemical researches and industrial applications. The lack of the structure of both CESH[L] and CESH[D] will further limit the engineering studies of both enzymes.

In this paper, we report high yield expressions and one-step purifications of two recombinant CESHs, including one CESH[D] and one CESH[L] using synthesized genes with optimized codons for *E. coli*. The properties and kinetics parameters of both recombinant enzymes were studied. The structure models of both CESH[L] and CESH[D] were constructed by homology modeling. Our results provide the basis for future biochemical, structural, and engineering studies of CESHs, and will be helpful to the industrial applications of both recombinant enzymes.

2 Materials and Methods

2.1 Gene Codon Optimization and Cloning

The two genes encoding CESH[D] (GeneBank: EU053208) (MW: 32,478.8) from *Bordetella* sp. BK-52 and CESH[L] (GeneBank: DQ471957) (MW: 28,136.5) from *Rhodococcus opacus* were optimized for codon adaption in *E. coli* by the

web server Jcat (<http://www.jcat.de/>) [12]. The original and optimized genes were shown in supplementary Figure S1. The genes were synthesized (Biomed Inc., Beijing) and cloned into the plasmid pET28a between the *Nde*I and *Eco*RI restriction sites, generating plasmids pET28a-CESH[D] and pET28a-CESH[L], respectively. The products of the constructs contain an N-terminal His₆-tag to facilitate the protein purification.

2.2 Protein Expression and Purification

The plasmids pET28a-CESH[D] and pET28a-CESH[L] were transformed into *E. coli* BL21(DE3), respectively. The cells were cultured in LB medium containing 100 mg/L of kanamycin at 37 °C until the optical density at 600 nm (OD₆₀₀) reached 0.6–0.8. The cells were then cultured at 16 °C for 30 min. After addition of 0.1 mM isopropyl β -D-1-thiogalactopyranoside, the culture was incubated at 16 °C for 24 h to induce the protein expression. And then the cells were harvested by centrifugation at 3,300 g. The cell pellets were suspended in buffer A (20 mM sodium phosphate buffer, 500 mM NaCl, 20 mM imidazole, pH 7.8) and lysed by ultrasonication. The supernatants were applied onto a Ni affinity column (GE Healthcare). The proteins were eluted with buffer B (20 mM sodium phosphate buffer, 500 mM NaCl, 500 mM imidazole, pH 6.0). The eluted fractions were dialysed against buffer C (137 mM NaCl, 2.7 mM KCl, 10 mM Na₂HPO₄, 2 mM KH₂PO₄, pH 7.5) three times. The purified proteins were stored at –20 °C in 50 % (v/v) glycerol. The protein purity was checked by SDS-PAGE. The protein concentrations were measured by the Bradford method [5].

2.3 Activity Measurement

To measure the CESH[D] activity, 0.1 mL enzyme solution was added into 0.9 mL 60 mM disodium *cis*-epoxysuccinate in 50 mM sodium phosphate buffer, pH 7.5. To measure the CESH[L] activity, 0.02 mL enzyme solution was added into 0.98 mL 1.0 M disodium *cis*-epoxysuccinate in 200 mM sodium phosphate buffer, pH 8.0. The solutions were incubated at 37 °C for 30 min and 20 min for CESH[D] and CESH[L], respectively, and the reactions were terminated by adding 0.4 mL 1.0 M H₂SO₄. The tartaric acids generated in the reactions were measured by the ammonium metavanadate method [18]. Briefly, 1 mL of 1 % (w/v) ammonium metavanadate was added into the reaction solution, and the solution was diluted to 10 mL. After a lapse of 5 min, the absorbance at 480 nm was measured on a Synergy HT Multi-mode microplate reader (BioTek Instruments, Inc.). The concentration of tartaric acid in the reaction solution was then calculated according to the standard curve recorded at various tartaric acid

concentrations. One unit of enzyme was defined as the amount of enzyme that generates 1 μmol of D(–)- or L(+)-tartaric acid per minute under the above conditions.

2.4 Effects of pH, Temperature and Substrate Concentration on the Activity

To detect the effect of pH, the activities of both enzymes were measured at various pH values from 4.0 to 11.0. The pH was adjusted by the addition of NaOH or H_3PO_4 and measured by a Sartorius PB-10 pH meter. To detect the effect of temperature, the activities were measured at various temperatures from 4 $^\circ\text{C}$ to 65 $^\circ\text{C}$. To detect the kinetics parameters of the catalytic reactions, the enzyme activities were assayed at substrate concentrations from 3.6 to 22.8 mM for the enzyme CESH[D], and from 10 to 100 mM for the enzyme CESH[L], respectively. The concentrations of CESH[D] and CESH[L] were 1.07 and 0.35 μM , respectively. The K_m and k_{cat} values were obtained by the Lineweaver–Burk plotting method [17].

2.5 Homology Modeling

The homolog sequences of CESH[L] and CESH[D] were obtained by Blast search against Protein Data Bank (PDB). MODELLER version 9.9 [24] was used to construct the homology models. Structures with PDB codes 1QO5, 2NO4, and 2HSZ were used as the templates of CESH[L]. Structures with PDB codes 2Y7T, 3LOT, and 3E49 were used as the templates of CESH[D]. Secondary structure predictions were made on the PSIPRED server (<http://bioinf.cs.ucl.ac.uk/psipred/>) [6].

3 Results and Discussion

3.1 Enzyme Purification

The recombinant genes of CESH[D] and CESH[L] were codon-optimized for expression in *E. coli*. The optimizations changed the codons of 58.5 % (172/294) and 59.3 % (150/253) residues of CESH[D] and CESH[L], respectively. The recombinant genes were expressed in *E. coli* at a very high level. High yields were helpful to purification, and one-step purifications by Ni column produced high pure enzymes (Fig. 2). The high yields and simple purification steps resulted in high recovery ratios (Table 1). The specific activities of crude enzymes for CESH[D] and CESH[L] were 11.4 and 95.8 U/mg, respectively, and after purification 94.9 % and 89.6 % recoveries were obtained for CESH[D] and CESH[L], respectively. As a comparison, the yield of CESH[D] in *Bordetella* sp. BK-52 was 1.8 U/mg specific activity for crude enzyme, and only 27.1 %

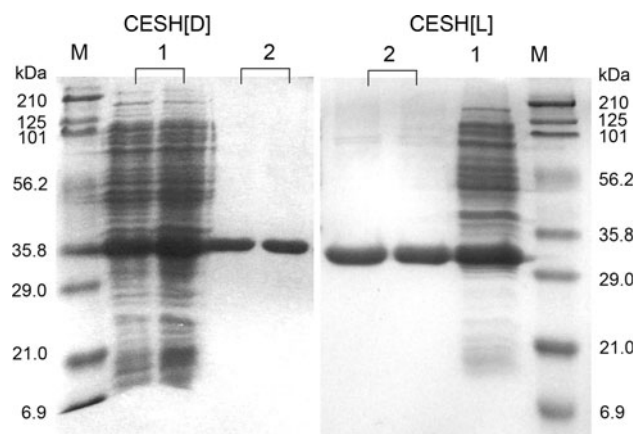


Fig. 2 SDS-PAGE of CESH[D] (left) and CESH[L] (right) at different purification steps stained with Coomassie Brilliant Blue G250. 5 μL samples containing $\sim 1 \mu\text{g}$ purified protein or $\sim 3 \mu\text{g}$ crude extract were loaded onto the gels. Lane M: protein marker; lane 1: crude extract; lane 2: purified protein

recovery was obtained after purification [21]; the yield of CESH[L] in *R. opacus* was 2.02 U/mg specific activity for crude enzyme, and only 9.6 % recovery was obtained after purification [19]. Therefore, our protocol provides simple and efficiently method to produce recombinant CESHs with high yield and recovery.

The recombinant protein yields from 250 mL culture were 41.0 and 48.7 mg for CESH[D] and CESH[L], respectively. The purified enzymes had specific activity 36.2 U/mg and 298.4 U/mg for CESH[D] and CESH[L], respectively, therefore the total activities of purified proteins from 250 mL culture were 1,483 U and 14,517 U for CESH[D] and CESH[L], respectively. The high yields of recombinant enzymes will facilitate the mechanism and structural studies.

3.2 Characterization of the Recombinant Enzymes

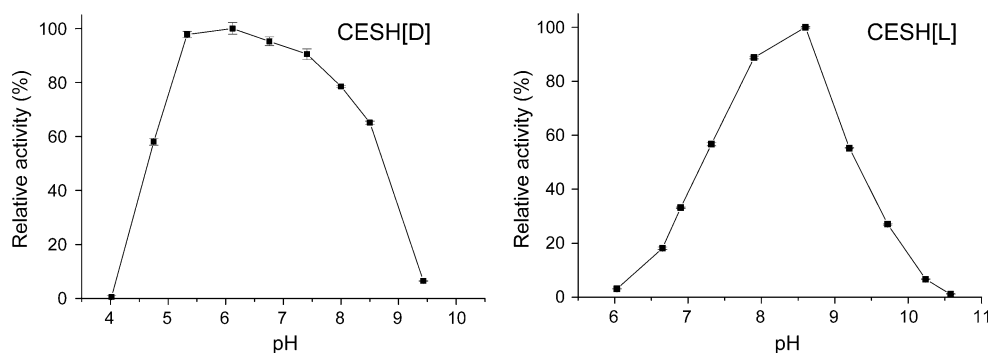
In order to get the properties of the recombinant enzymes, we measured the effects of pH and temperature on their activities. We also measured the kinetics parameters of both enzymes to compare the enzymatic reaction mechanisms.

The optimal pHs were obtained by the activity measurements at pH from 4.0 to 11.0 (Fig. 3). CESH[D] showed an optimal pH of 6.0, and had high activities (>60 %) from pH 5.5 to 8.5. CESH[L] showed an optimal pH of 8.5, and had high activities (>60 %) from pH 7.5 to 8.5. These results indicated that CESH[D] has a broader pH stability than CESH[L], and are in agreement with the previous reported results for native enzymes purified from the original species [19, 21].

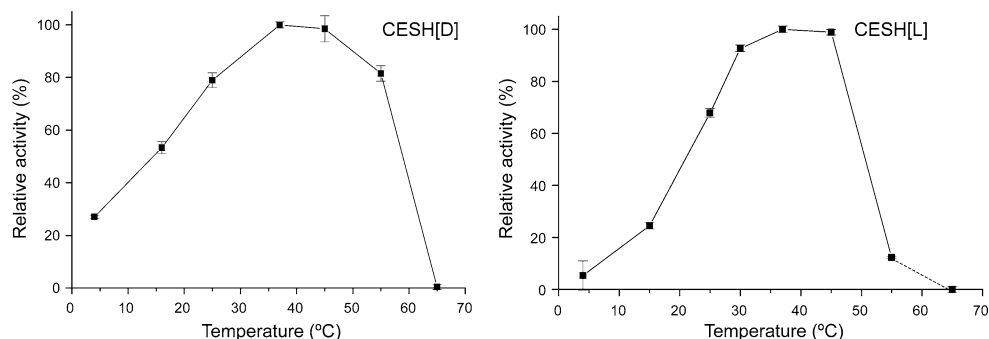
The optimal temperatures were obtained by the activity measurements at 4–65 $^\circ\text{C}$ (Fig. 4). Results showed that both CESH[D] and CESH[L] have similar optimal temperatures

Table 1 Summary of the purifications of CESH[D] and CESH[L] from 250 mL LB cultures

Purification process	Total Protein (mg)	Total activity (U)	Specific activity (U/mg)	Purification fold	Recovery (%)
CESH[D]					
Crude extract	137.7	1,563	11.4	1	100
Purified enzyme	41.0	1,483	36.2	3.189	94.9
CESH[L]					
Crude extract	169.1	16,200	95.8	1	100
Purified enzyme	48.7	14,517	298.4	3.114	89.6

**Fig. 3** Effect of pH on the activities of purified CESH[D] (*left*) and CESH[L] (*right*) at 37 °C. The buffer for CESH[D] contained 60 mM disodium *cis*-epoxysuccinate, 50 mM sodium phosphate buffer, and the buffer for CESH[L] contained 1.0 M disodium *cis*-epoxysuccinate, 200 mM sodium phosphate buffer. The pHs were adjusted by the addition of NaOH or H₃PO₄. The reaction time were 30 min for

CESH[D] and 20 min for CESH[L]. The concentrations of CESH[D] and CESH[L] are 1.07 μ M and 0.35 μ M, respectively. The highest activity of CESH[D] which refers to 100 % is 43.3 U/mg specific activity at pH 6.12. The highest activity of CESH[L] which refers to 100 % is 316.1 U/mg specific activity at pH 8.6

**Fig. 4** Effect of temperature on the activities of purified CESH[D] (*left*) and CESH[L] (*right*). The buffer for CESH[D] contained 60 mM disodium *cis*-epoxysuccinate, 50 mM sodium phosphate buffer, pH 7.5. The buffer for CESH[L] contained 1.0 M disodium *cis*-epoxysuccinate, 200 mM sodium phosphate buffer, pH 8.0. The reaction time were 30 min for CESH[D] and 20 min for

CESH[L]. The concentrations of CESH[D] and CESH[L] are 1.07 and 0.35 μ M, respectively. The highest activity of CESH[D] which refers to 100 % is 37.2 U/mg specific activity at 37 °C. The highest activity of CESH[L] which refers to 100 % is 271.7 U/mg specific activity at 45 °C

of 40–45 °C. The result for CESH[D] is in agreement with the previous reported result for native enzyme purified from the original specie, but the recombinant CESH[L] showed a higher optimal temperature than the reported value (20–30 °C) of native enzyme purified from the original species.

With *cis*-epoxysuccinic acid as the substrate, the K_m and k_{cat} values of the enzymes were determined at pH 7.5 and

37 °C by the Lineweaver–Burk plotting method (Fig. 5). The values of K_m , k_{cat} and k_{cat}/K_m are shown in Table 2. The K_m value of CESH[D] is slightly larger than that of CESH[L], but the k_{cat} value of CESH[D] is only about one-fifth of that of CESH[L]. Therefore, the k_{cat}/K_m value of CESH[D] is about one-fifth of that of CESH[L]. The similar K_m values for both enzymes indicate that both enzymes bind *cis*-epoxysuccinate with similar affinities. However,

Fig. 5 Lineweaver-Burk plots of CESH[D] (left) and CESH[L] (right). The effect of substrate concentration on the two types of CESHs were determined at different concentration over the range of 3.6–22.8 mM for CESH[D] and 10–100 mM for CESH[L], and the reaction time were 30 min for CESH[D] and 20 min for CESH[L] at 37 °C. The concentrations of CESH[D] and CESH[L] are 1.07 and 0.35 μ M, respectively

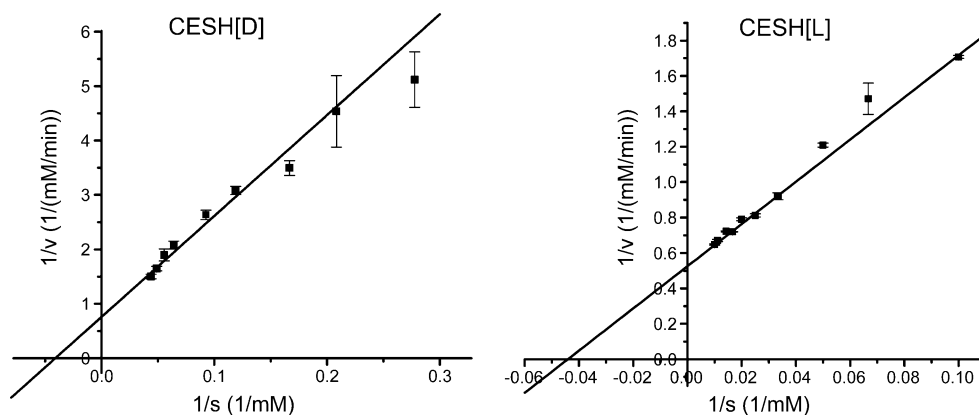


Table 2 Kinetics parameters of the hydrolysis of *cis*-epoxysuccinic acid by CESH[D] and CESH[L]

	K_m (mM)	k_{cat} (min^{-1})	k_{cat}/K_m ($\text{mM}^{-1} \text{min}^{-1}$)
CESH[D]	24.4	1.23×10^3	50.4
CESH[L]	22.7	5.44×10^3	239.8

the large difference of k_{cat}/K_m values indicates that the efficiency of CESH[D] is much lower than that of CESH[L]. Since both D(−)- and L(+)-tartaric acids are important building blocks in the pharmaceutical and food industries, the mechanism difference should be studied in future to increase the efficiency of CESH[D].

3.3 Homology Modeling of CESH[L] and CESH[D]

CESH[D] and CESH[L] catalyze the same substrate, *cis*-epoxysuccinate, to form different enantiomeric tartaric acids. The catalytic mechanisms are interested by lots of researchers, and our data indicated that the efficiency of CESH[D] is much lower than that of CESH[L] although both enzymes have similar affinity to the substrates. The structure of the enzymes may be helpful to understand the underlying mechanism difference but the structures of the two CESHs have not been reported yet. To get structural insight into the two enzymes, we constructed structural models of CESH[L] and CESH[D] by homology modeling using MODELLER9.9 [24].

By search in Protein Data Bank using Blast, several proteins with low homology with each of the CESHs were found and used as templates in the modeling (Supplementary Figure S2). Because the sequence identities between the CESHs and the candidate templates are low (24–34 %), multiple templates were used in the homology modeling to get more reliable results [8, 10, 14]. The templates for CESH[L] include L-2-haloacid dehalogenase from *Xanthobacter autotrophicus* GJ10 (PDB code 1QQ5, 27 % identity in 209 residues), haloacid dehalogenase DehIVa from *Burkholderia cepacia* MBA4 (PDB code

2NO4, 34 % identity in 117 residues) and a novel predicted phosphatase from *Haemophilus somnus* (PDB code 2HSZ, 24 % identity in 232 residues). The templates for CESH[D] are 3-keto-5-aminohexanoate cleavage enzyme (Kce) from *Candidatus Cloacamonas acidaminovorans* (PDB code 2Y7D, 27 % identity in 299 residues) and two uncharacterized proteins from *Archaeoglobus fulgidus* (PDB code 3LOT, 30 % identity in 292 residues) and *Burkholderia xenovorans* LB400 (PDB code 3E49, 26 % identity in 287 residues). The templates of CESH[L] and CESH[D] belong to α/β -hydrolase fold and TIM barrel fold, respectively. Both folds are widespread in various proteins with divergent functions [20, 27], which is the reason why the functions of some templates are not CESH-related enzymes. To confirm the reliability of the models based on low-identity templates, the secondary structures of the two CESHs were predicted from the sequences. The predicted secondary structures correlated well with the secondary structure compositions in both structural models (Supplementary Figure S3), which confirmed the high reliabilities of these models.

The model of CESH[L] adopts a typical α/β -hydrolase fold with a cap domain and a core domain (Fig. 6a), which extensively presents in epoxide hydrolases. A unique characteristic among epoxide hydrolases is that although they commonly have low sequential similarities, their catalytic residues remain conserved. Based on previous studies, the catalytically important residues of L-2-haloacid dehalogenase [23] and DehIVa [22, 25] were indicated by asterisk (*) in supplementary Figure S2; almost all of these residues were conserved in CESH[L]. The existence of conserved catalytically important residues in CESH[L] (Asp18, Thr22, Arg55, Thr133, Lys164, Tyr170 and Asp193), which may consist a catalytic pocket at the interface of two functional domains (Fig. 6a), indicated that CESH[L] may adopt a similar catalytic mechanism as L-2-haloacid dehalogenase or DehIVa.

The model of CESH[D] possesses a unique TIM barrel fold composed of 8 α -helices and 8 β -strands, and 2 extra

Fig. 6 Ribbon representation of structural models of CESH[L] (a) and CESH[D] (b). Side chains of conserved catalytically important residues were indicated in red, Zn^{2+} ion was indicated as blue ball

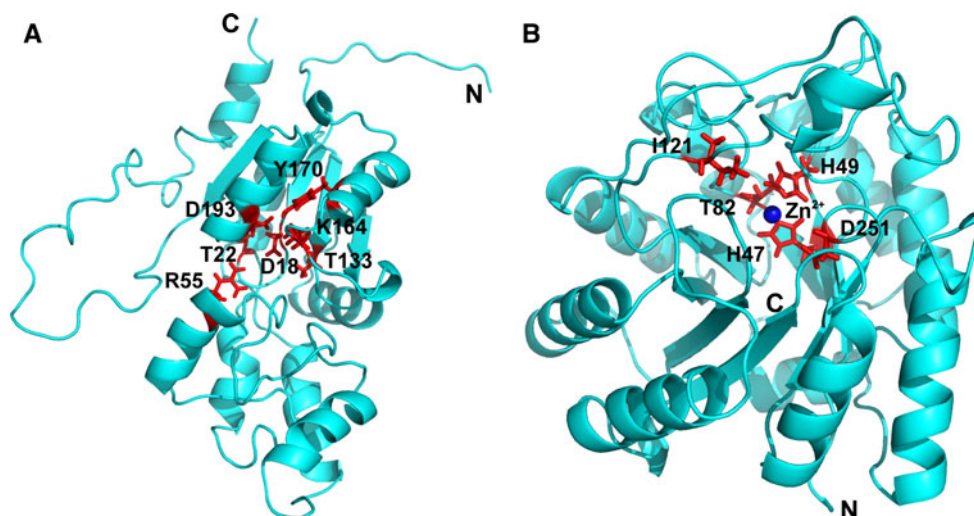


Table 3 The relative activities of CESH[D] in the presence of EDTA (10 mM) or various metal ions (50 mM)

CESH[D]	+	+	+	+	+	+	+	+	—
EDTA	—	—	—	—	+	+	+	+	—
Ca ²⁺	—	+	—	—	—	+	—	—	—
Mg ²⁺	—	—	+	—	—	—	+	—	—
Zn ²⁺	—	—	—	+	—	—	—	+	—
Activity (%)	100 ± 3.8	99.6 ± 1.8	95.6 ± 12.2	94.8 ± 4.6	8.2 ± 1.5	26.9 ± 4.3	57.7 ± 4.7	91.9 ± 3.8	0

The specific activity of CESH[D] without additive was 26.2 U/mg which was normalized as 100 %

short α -helices exist on the top and bottom of the barrel, respectively (Fig. 6b). A zinc ion may present near the catalytic site (Fig. 6b). CESH[D] only preserved part of the catalytically important residues of one modeling template, 3-keto-5-aminohexanoate cleavage enzyme Kce [3] (Fig. 2b, His47, His49, Thr82, Ile121 and Asp251). This is reasonable because CESH[D] and Kce have different enzymatic functions. The fold conservation suggests they may share an ancestor, while the active sites were evolved to have different functions. All templates used in modeling for CESH[D] contain a zinc ion, and the zinc ion participates the catalytic process of enzyme Kce. Therefore, we speculated CESH[D] may also contain a divalent metal ion. We first checked the activity in the presence of 10 mM EDTA and found CESH[D] almost lost its activity (Table 3). Then we added 50 mM excess divalent metal ions in the EDTA-treated samples, and we found that the activities of CESH[D] were restored. Further, zinc ion can restore the activity to ~100 %, while other ions only restore the activity partially (Table 3). These results confirmed that the active CESH[D] contains a divalent metal ion, preferred to be zinc, which is necessary for its activity.

Our studies indicated CESH[L] and CESH[D] have distinct structures as well as catalytically important residues, suggesting totally different catalytic mechanisms. To reveal the mechanisms of CESHs, high-resolution 3D-structures

and detailed functional researches were indispensable. Discoveries presented here will provide clues for further structural and functional studies.

Previous studies suggested that pure epoxide hydrolases have low stability which prevented the direct industrial application of the enzyme [19]. Protein engineering may help to increase the stability, but the stability could not be carefully and extensively studied without high yield enzyme production. Our protocol for production of recombinant CESHs has a high yield and the recombinant enzymes have similar properties to the native enzymes. Further, the structural models of the two enzymes could provide clues for the protein engineering studies. Therefore, our works provide the basis to the stability and protein engineering studies, which will be helpful to the industrial recombinant enzyme productions and other industrial applications.

4 Conclusions

In this paper, both CESH[D] and CESH[L] were recombinantly expressed in *E. coli* with high yield and recovery. We successfully used codon-optimized synthesized genes and His₆-tag fusion protein to obtain high expression and fast purification. The purified recombinant proteins exhibited

similar properties as the native proteins purified from the original species, and the only exception is that the recombinant CESH[L] showed a slightly higher optimal temperature than that of native CESH[L]. This indicated the fusion His₆-tags have little effect on the enzyme activity and property. Therefore, purified recombinant enzymes can be used in the future biochemical and structural studies. Homology modeling of the two CESHs indicates that CESH[L] and CESH[D] have completely different structures and active site residues. CESH[L] adopted a typical α/β -hydrolase fold with a cap domain and a core domain, and conserved catalytically important residues consist a catalytic pocket at the interface of two functional domains. CESH[D] possessed a unique TIM barrel fold composed of 8 α -helices and 8 β -strands, and 2 extra short α -helices exist on the top and bottom of the barrel, respectively. A divalent metal ion was found in CESH[D] by homology modeling and activity experiments. The metal ion, preferred to be zinc, is necessary to the activity of CESH[D]. Our work provides the basis to the stability and protein engineering studies, as well as the structural insight of the catalytic mechanisms of the two CESHs, which will be helpful to the industrial productions and other applications.

Acknowledgments This work is supported by One-hundred-Talented-People program (KSCX2-YW-G-066) from the Chinese Academy of Sciences, and the National Natural Science Foundation of China (Grant No. 30970050).

References

1. Archelas A, Furstoss R (1998) *Trends Biotechnol* 16:108–116
2. Archelas A, Furstoss R (2001) *Curr Opin Chem Biol* 5:112–119
3. Bellinzoni M, Bastard K, Perret A, Zaparucha A, Perchat N, Vergne C, Wagner T, de Melo-Minardi RC, Artiguenave F, Cohen GN, Weissenbach J, Salanoubat M, Alzari PM (2011) *J Biol Chem* 286:27399–27405
4. Besse P, Veschambre H (1994) *Tetrahedron* 50:8885–8927
5. Bradford MM (1976) *Anal Biochem* 72:248–254
6. Buchan DWA, Ward SM, Lobley AE, Nugent TCO, Bryson K, Jones DT (2010) *Nucleic Acids Res* 38:W563–W568
7. Bucko M, Vikartovska A, Lacik I, Kollarikova G, Gemeiner P, Patoprsty V, Brygin M (2005) *Enzyme Microb Technol* 36:118–126
8. Cheng JL (2008) *BMC Struct Biol* 8:18
9. Choi WJ (2009) *Appl Microbiol Biotechnol* 84:239–247
10. Fernandez-Fuentes N, Rai BK, Madrid-Aliste CJ, Fajardo JE, Fiser A (2007) *Bioinformatics* 23:2558–2565
11. Ghosh AK, Koltun ES, Bilcer G (2001) *Synthesis-Stuttgart* 2001:1281–1301
12. Grote A, Hiller K, Scheer M, Munch R, Nortemann B, Hempel DC, Jahn D (2005) *Nucleic Acids Res* 33:W526–W531
13. Jaeger KE, Eggert T, Eipper A, Reetz MT (2001) *Appl Microbiol Biotechnol* 55:519–530
14. Larsson P, Wallner B, Lindahl E, Elofsson A (2008) *Protein Sci* 17:990–1002
15. Lee EY, Shuler ML (2007) *Biotechnol Bioeng* 98:318–327
16. Li X, Xu TC, Lu HB, Ma XH, Kai L, Guo KP, Zhao YH (2010) *Protein Expr Purif* 69:16–20
17. Lineweaver H, Burk D (1934) *J Am Chem Soc* 56:658–666
18. Liu YQ, Yan XK, Zhou WL, Pan ZM, Zhang JP (1983) *Ind Microbiol* 13:32–37
19. Liu ZQ, Li Y, Xu YY, Ping LF, Zheng YG (2007) *Appl Microbiol Biotechnol* 74:99–106
20. Nagano N, Orengo CA, Thornton JM (2002) *J Mol Biol* 321:741–765
21. Pan HF, Bao WN, Xie ZP, Zhang JG, Li YQ (2010) *J Microbiol Biotechnol* 20:659–665
22. Pang BCM, Tsang JSH (2001) *FEMS Microbiol Lett* 204:135–140
23. Ridder IS, Rozeboom HJ, Kalk KH, Dijkstra BW (1999) *J Biol Chem* 274:30672–30678
24. Sali A, Blundell TL (1993) *J Mol Biol* 234:779–815
25. Schmidberger JW, Wilce JA, Tsang JSH, Wilce MCJ (2007) *J Mol Biol* 368:706–717
26. Steinreiber A, Faber K (2001) *Curr Opin Biotechnol* 12:552–558
27. Widersten M, Gurell A, Lindberg D (2010) *Biochim Biophys Acta* 1800:316–326
28. Willaert R, De Vuyst L (2006) *Appl Microbiol Biotechnol* 71:155–163